

Two-State Allosteric Behavior in a Single-Domain Signaling Protein

Brian F. Volkman,^{1*} Doron Lipson,² David E. Wemmer,³
Dorothee Kern^{2†}

Protein actions are usually discussed in terms of static structures, but function requires motion. We find a strong correlation between phosphorylation-driven activation of the signaling protein NtrC and microsecond time-scale backbone dynamics. Using nuclear magnetic resonance relaxation, we characterized the motions of NtrC in three functional states: unphosphorylated (inactive), phosphorylated (active), and a partially active mutant. These dynamics are indicative of exchange between inactive and active conformations. Both states are populated in unphosphorylated NtrC, and phosphorylation shifts the equilibrium toward the active species. These results support a dynamic population shift between two preexisting conformations as the underlying mechanism of activation.

The heart of signal transduction is the switching of proteins between inactive and active states. This process can be promoted by other proteins, domains, ligands, or covalent modifications such as phosphorylation. A central question is how these effectors lead to a change in activity. Two models have classically been discussed: (i) the effector induces a new structure or (ii) shifts a preexisting equilibrium. The second model is also known as allosteric activation, a shift between relaxed (R) and tense (T) states (*1, 2*), a model also known as allosteric activation. Although allostery is well accepted for multidomain proteins, for regulation within a single domain, the induced-fit mechanism is still widely held. In particular, phosphorylation that regulates signal transduction pathways is usually assumed to trigger a conformational switch. The idea of inducing a new structure is based on the traditional assumption of unique folds dictated by protein sequence. Modern concepts of protein-folding funnels and energy landscapes (*3, 4*), which describe folded proteins as an ensemble of conformational substates, challenge traditional concepts of the control of protein activity (*5, 6*). According to this statistical viewpoint, protein function is not determined purely by the static structure but rather through a redistri-

bution of already existing populations in response to changes in environment. There is little experimental data that discriminates between induced-fit and population-shift models because the conformational changes are fast and the populations are often strongly skewed. Our data on the nitrogen regulatory protein C (NtrC) provide direct experimental evidence for a population-shift mechanism in this phosphorylation-regulated signaling protein.

NtrC is a member of the “two-component system” signaling family (*7*). Two highly conserved components, histidine kinases and response regulators, control gene expression, chemotaxis, antibiotic resistance, and many other bacterial processes. The “receiver domain” of the response regulators is the molecular switch, which is controlled by phosphorylation of an active-site aspartate. In NtrC, phosphorylation of the receiver domain results in large structural changes (*8*). The active conformation of the receiver domain is essential for oligomerization of full-length NtrC, which then promotes transcription by the σ^{54} -holoenzyme form of RNA polymerase (*9*). NtrC variants with partial activity in the absence of phosphorylation show nuclear magnetic resonance (NMR) chemical shift differences (*10*) in the same area that changes structure upon phosphorylation. Each mutant displayed evidence of conformational heterogeneity rather than adopting a unique, partially active conformation. To shed light on the mechanism of activation, we characterized at atomic resolution the molecular motion of the NtrC receiver domain in three different functional states.

NMR relaxation of backbone amides provides a powerful experimental approach for detecting conformational dynamics of proteins at atomic resolution (*11*). Three relax-

ation parameters were measured for all backbone amide nitrogens of the regulatory domain of NtrC (NtrC^r): ¹H-¹⁵N nuclear Overhauser effect (NOE), rate constants for spin-lattice relaxation (*R*₁), and spin-spin relaxation (*R*₂) (Fig. 1) (*12*). The experiments were performed for NtrC^r in three different functional states: the inactive unphosphorylated form NtrC^r, a partially active mutant form NtrC^r [Asp⁸⁶ → Asn⁸⁶/Ala⁸⁹ → Thr⁸⁹ (D86N/A89T)], and the fully active phosphorylated form P-NtrC^r (*13*). The NMR spectra for P-NtrC^r were acquired during steady-state autophosphorylation/dephosphorylation using carbamoylphosphate and Mg²⁺ as substrates for the enzyme turnover (*8*), because of the short lifetime of the phosphorylated form.

To extract internal backbone dynamics, relaxation parameters (Fig. 1) were analyzed using an extended Lipari-Szabo “model-free” approach (*14, 15*), which allows the characterization of complex internal dynamics over a broad range of time scales (*16*). Fast (pico- to nanosecond) motions of the N-H bond vector, expressed in terms of an order parameter (*S*²) ranging from 0 (unrestricted) to 1 (completely restricted), are comparable for all three forms of NtrC^r (Fig. 2A). The key for monitoring the activation process is the micro- to millisecond time-scale motions (Figs. 2B and 3, A through C) identified by the exchange term *R*_{ex}, which indicates conformational exchange between conformations that sense different chemical environments. The value of *R*_{ex} is directly proportional to the difference in chemical shift between the exchanging species and not necessarily to the magnitude of structural change. Therefore, those amides with *R*_{ex} values beyond detection reflect a large difference in chemical shift between the exchanging species.

The two central results are illustrated in Fig. 3: First, many residues of unphosphorylated wild-type (Fig. 3A) and active mutant NtrC^r (D86N/A89T) (Fig. 3B) show prominent micro- to millisecond time-scale motions that disappear in the phosphorylated form (Fig. 3C). In addition to the fitted values for *R*_{ex}, several residues are indicated with *R*_{ex} values ≥ 20 s⁻¹ (Figs. 2B and 3, A through C). Those residues could not be detected because of large line-widths from exchange broadening. Second, dynamic regions in both unphosphorylated forms (Fig. 3, A and B) map precisely to the region that experiences a structural change upon activation (Fig. 3, D and E). This suggests that the conformational exchange that is observed between the inactive and active conformations (*17*).

How are these microsecond time-scale motions related to function? Our dynamic data are not consistent with a model for activation where NtrC^r exists in the inactive

¹National Magnetic Resonance Facility at Madison (NMRFAM), Department of Biochemistry, University of Wisconsin-Madison, Madison, WI 53706, USA.

²Department of Biochemistry, Brandeis University, Waltham, MA 02454, USA. ³Physical Biosciences Division, Lawrence Berkeley National Laboratory and Department of Chemistry, University of California, Berkeley, CA 94720, USA.

*Present address: Department of Biochemistry, Medical College of Wisconsin, Milwaukee, WI 53226, USA.

†To whom correspondence should be addressed. E-mail: dkern@brandeis.edu

REPORTS

conformation (*I*) and phosphorylation induces a change in structure to the active conformation (*A*) (Fig. 3A). Previously, we showed that the size of chemical shift differences between a series of mutants relative to wild-type NtrC^r strongly correlated with the level of transcriptional activity (Fig. 4) (10). We proposed that the activating mutations may cause a shift in population toward the active state, a model that has been suggested for response regulators (18–20). This model is buttressed by the dynamics here: resonances showing large shift differences also show microsecond time-scale motions and map exactly to the switch region (Fig. 3). In contrast, amides in the other parts of the molecule, which do not undergo structural changes upon activation, show no motion on the slow time scale. Thus, the observed linear shifts (Fig. 4A) are due to a conformational exchange between *I* and *A*, which is fast on the NMR time scale. This results in an average signal with the peak position determined by the relative populations of the exchanging conformers; larger chemical shift changes occur as *A* becomes more populated (Fig. 4).

The key question remains: how does wild-type NtrC^r get to the activated state? Surprisingly, wild-type NtrC^r undergoes a conformational exchange process in exactly the same area as the mutants (Fig. 3, A and B). In addition, the shifts of residues showing exchange in wild-type NtrC^r are collinear with those detected for the mutants (Fig. 4A). Consequently, *I* and *A* already coexist in unphosphorylated NtrC^r, with the equilibrium skewed toward *I*. After phosphorylation, conformational exchange virtually disappears (Fig. 3C), suggesting that the equilibrium is far shifted toward the active conformation (>99%). The population of active species in wild-type, unphosphorylated NtrC^r can be estimated to be between 2 and 10% because we were able to solve the structure by NMR. The ¹H–¹H NOE intensities in the region of conformational change were comparable to those observed for P-NtrC^r, which populates the active form almost exclusively. In contrast, NOE spectra on the double mutant resulted in a loss of NOEs in the region of conformational exchange. The inactive conformation must therefore be the dominant species in wild-type NtrC^r, with the active conformation populated to at least 2% to yield the observed R_{ex} values. Consequently, the position of the average signals in Fig. 4B reflects the approximate equilibrium constants between *I* and *A* for all forms. An equilibrium constant of about 1 can be determined for NtrC^r (D86N/A89T) (21). Phosphorylation of this mutant form increases its activity only to that of the phosphorylated wild type and results in chemi-

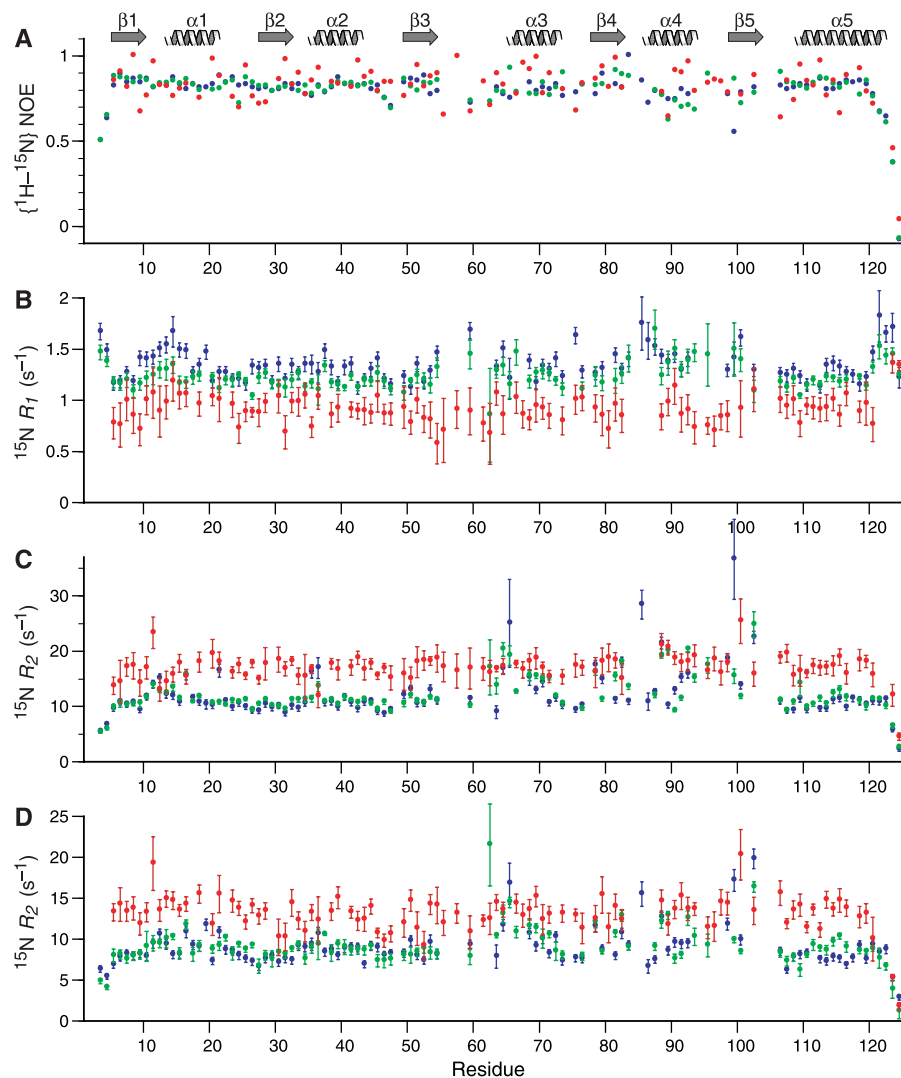


Fig. 1. Backbone ¹⁵N relaxation parameters for NtrC^r, NtrC^r(D86N/A89T), and P-NtrC^r are shown in blue, green, and red, respectively. Results of (A) {¹H–¹⁵N} NOE, (B) ¹⁵N R_1 , and (C) ¹⁵N R_2 measurements at 750 MHz ¹H frequency and (D) ¹⁵N R_2 at 600 MHz are plotted as a function of residue number. The approximate locations of secondary structure elements are indicated above. Values for backbone amide signals are unavailable for six prolines at positions 48, 58, 74, 77, 103, and 105, as well as the two NH₂-terminal residues. Additional residues were excluded from the relaxation and model-free analysis because of spectral overlap or extreme line-broadening. The significantly increased R_1 , and decreased R_2 values for P-NtrC^r compared to the unphosphorylated forms is caused by the high-salt conditions required to maintain phosphorylation (8).

cal shifts identical to P-NtrC^r, supporting the population shift model. In summary, NtrC^r interconverts between the two functionally important conformers and not among many random substates. Phosphorylation does not induce a new structure, but rather shifts a preexisting equilibrium.

If there is already a significant fraction of active molecules before phosphorylation, why is there no basal transcriptional activity and how can a sharp switch be accomplished? Oligomerization of full-length NtrC is essential for biological output (22). The active conformation of NtrC's receiver domain triggers oligomerization through interaction with the central domain. Therefore, the activity for full-length NtrC is highly sigmoidal in con-

centration (23), ensuring a sharp signal response. Our data suggest that the population of active conformers in NtrC^r is below the response threshold. In contrast, the single-domain response regulator CheY, which does not oligomerize upon phosphorylation, shows a low level of activity in the unphosphorylated state (24), directly reflecting the population of active conformers. In fact, microsecond time-scale motions have been reported for unphosphorylated CheY (25) and Spo0F (20), suggesting that the two-state exchange model might be true for response regulators in general. Our study of NtrC^r dynamics in three defined functional states, combined with knowledge of the inactive and active protein conformations, enables the direct observation

REPORTS

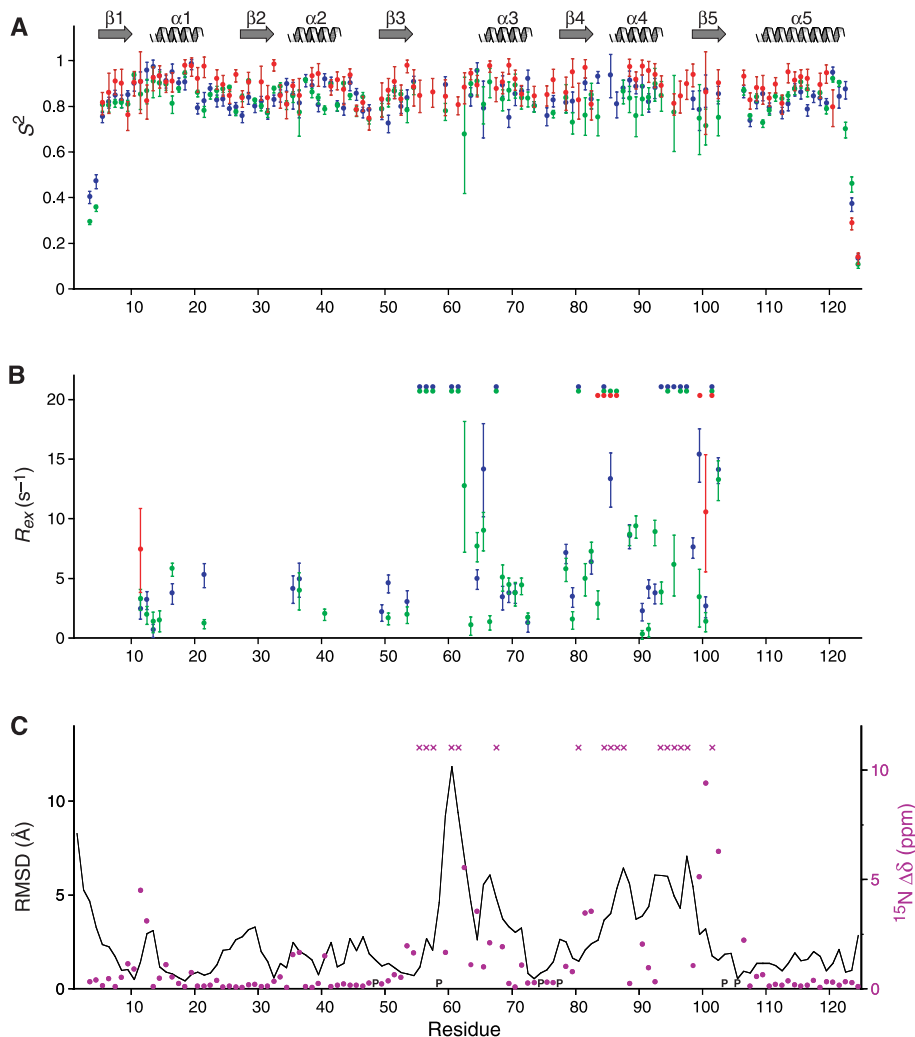


Fig. 2. Correlation between backbone dynamics parameters and conformational switch upon activation. Order parameters S^2 characterizing motions in the pico- to nanosecond time scale (A) and exchange values R_{ex} indicating motions in the micro- to millisecond time regime (B) deduced from model-free analysis of ^{15}N relaxation data (Fig. 1) are plotted as a function of residue number. Values for NtrC^r, NtrC^r(D86N/A89T), and P-NtrC^r are shown in blue, green, and red, respectively. R_{ex} values of 20 s⁻¹ are shown when extremely broad signals precluded the determination of relaxation parameters. (C) Backbone atomic RMS deviations (solid line) and backbone and ^{15}N chemical shift between NtrC^r and P-NtrC^r (purple dots). Displacements were measured using the NMR structures of NtrC^r and P-NtrC^r (8) superimposing residues 4 to 9, 14 to 53, and 108 to 121. A purple “X” reflects a ^{15}N chemical shift that was not determined in either NtrC^r or P-NtrC^r, where the missing resonance is presumed to be broadened beyond detection as the result of chemical exchange between two signals with large shift differences. Proline residues are indicated by “P” on the x axis.

of the functional equilibrium process. A movie presentation of the activation process can be found at (26).

The observation of persistent motion in the $\beta 4$ – $\alpha 4$ loop and part of $\beta 5$ in P-NtrC^r (Fig. 3C) might seem to contradict the basic idea of a two-state equilibrium. R_{ex} in the $\beta 4$ – $\alpha 4$ loop arises from unwinding the NH₂-terminal portion of helix 4 upon phosphorylation (8). A likely source of the persistent R_{ex} in β -strand 5 is motion of the side chain of Tyr¹⁰¹ (Y101). The dynamic behavior around Y101 in all three forms of NtrC^r indicates that the conformational exchange of this conserved aromatic side chain is not simply cou-

pled to the equilibrium between *I* and *A* described above (27). The combination of the relaxation and activity data allowed the discrimination between two modes of motion, one that is correlated to the activation process and a second, uncoupled motion.

Our NMR relaxation experiments demonstrate that activation of the NtrC regulatory domain occurs in the micro- to millisecond range, and not in pico- or nanoseconds, where the dynamics do not change between unphosphorylated and phosphorylated NtrC^r. In fact, functionally important protein motions are likely to be in this time regime because many biological processes

occur in micro- to millisecond time scales.

We propose that stabilization of preexisting conformations may be a fundamental paradigm for ligand binding. For calmodulin, a similar conformational exchange process was detected using NMR relaxation experiments (28, 29). Overall, the concept of “allosteric” regulation of single domains has not been widely considered. NMR provides a good tool to study conformational equilibria; however, to identify functionally important motions it is necessary to combine structural, dynamic, and functional information.

References and Notes

1. J. Monod, J. Wyman, J. Changeux, *J. Mol. Biol.* **12**, 88 (1965).
2. D. E. Koshland Jr., G. Nemethy, D. Filmer, *Biochemistry* **5**, 365 (1966).
3. C. M. Dobson, A. Sali, M. Karplus, *Angew. Chem. Int. Ed. Engl.* **37**, 868 (1998).
4. K. A. Dill, *Protein Sci.* **8**, 1166 (1999).
5. H. Frauenfelder, F. Parak, R. D. Young, *Annu. Rev. Biophys. Biophys. Chem.* **17**, 451 (1988).
6. S. Kumar, B. Ma, C. J. Tsai, N. Sinha, R. Nussinov, *Protein Sci.* **9**, 10 (2000).
7. J. B. Stock, M. G. Surette, M. Levitt, P. Park, in *Two-Component Signal Transduction*, J. A. Hoch, T. J. Silhavy, Eds. (American Society for Microbiology, Washington, DC, 1995), pp. 25–51.
8. D. Kern et al., *Nature* **402**, 894 (1999).
9. I. Rombel, A. North, I. Hwang, C. Wyman, S. Kustu, *Cold Spring Harbor Symp. Quant. Biol.* **63**, 157 (1998).
10. M. Nohaila, D. Kern, D. Wemmer, K. Stedman, S. Kustu, *J. Mol. Biol.* **273**, 299 (1997).
11. A. G. Palmer, *Curr. Opin. Struct. Biol.* **7**, 732 (1997).
12. All spectra were collected at 25°C on Bruker DMX spectrometers equipped with three-axis gradients and triple-resonance probeheads. Relaxation parameters were measured at 750.13 MHz (^{15}N R_1 , R_2 , and ^1H – ^{15}N NOE) and 600.13 MHz (R_2 only) ^1H frequency. All pulse schemes used gradients for sensitivity enhancement and selective pulses for water flip-back. Data for R_1 and R_2 measurements on NtrC^r and NtrC^r(D86N/A89T) were acquired with 16 scans per free induction decay (FID), 220 complex ^{15}N points, and 512 complex ^1H points. Data for R_1 and R_2 measurements on P-NtrC^r were acquired with 24 scans per FID, 160 complex ^{15}N points, and 512 complex ^1H points. Heteronuclear NOE measurements were acquired similarly, but with 24 and 48 scans per FID for the unphosphorylated and phosphorylated species, respectively. Spectral widths at 750 (600) MHz were 10,000 (8012.82) Hz in the ^1H dimension and 2222.22 (1778.09) Hz in the ^{15}N dimension. R_2 values were obtained with eight different durations of the delay T : 7.2, 14.4, 21.6, 28.8, 43.2, 57.6, 86.4, and 115.2 ms. R_1 values were obtained with $T = 10, 20, 60, 120, 200, 400, 800,$ and 1400 ms. Duplicate spectra were recorded for $T = 10$ and 400 ms (R_1) and $T = 7.2$ and 57.6 ms (R_2) for estimation of peak height uncertainties.
13. Uniformly ^{15}N -labeled NtrC^r and NtrC^r(D86N/A89T) were prepared as described (10). Sample conditions for NtrC^r and NtrC^r(D86N/A89T) were 50 mM sodium phosphate buffer, pH = 6.75, 0.9 mM protein concentration. Phosphorylated NtrC^r was prepared by autophosphorylation using 200 mM carbamoylphosphate, 50 mM MgCl₂, 200 mM sodium phosphate buffer, pH = 6.75, and 0.3 mM protein concentration (8).
14. G. Lipari, A. Szabo, *J. Am. Chem. Soc.* **104**, 4546 (1982).
15. G. M. Clore et al., *J. Am. Chem. Soc.* **112**, 4989 (1990).
16. Relaxation rates were obtained from Marquardt-Levenberg nonlinear fits to the decay curves using in-house software written in FORTRAN-77 and Perl.

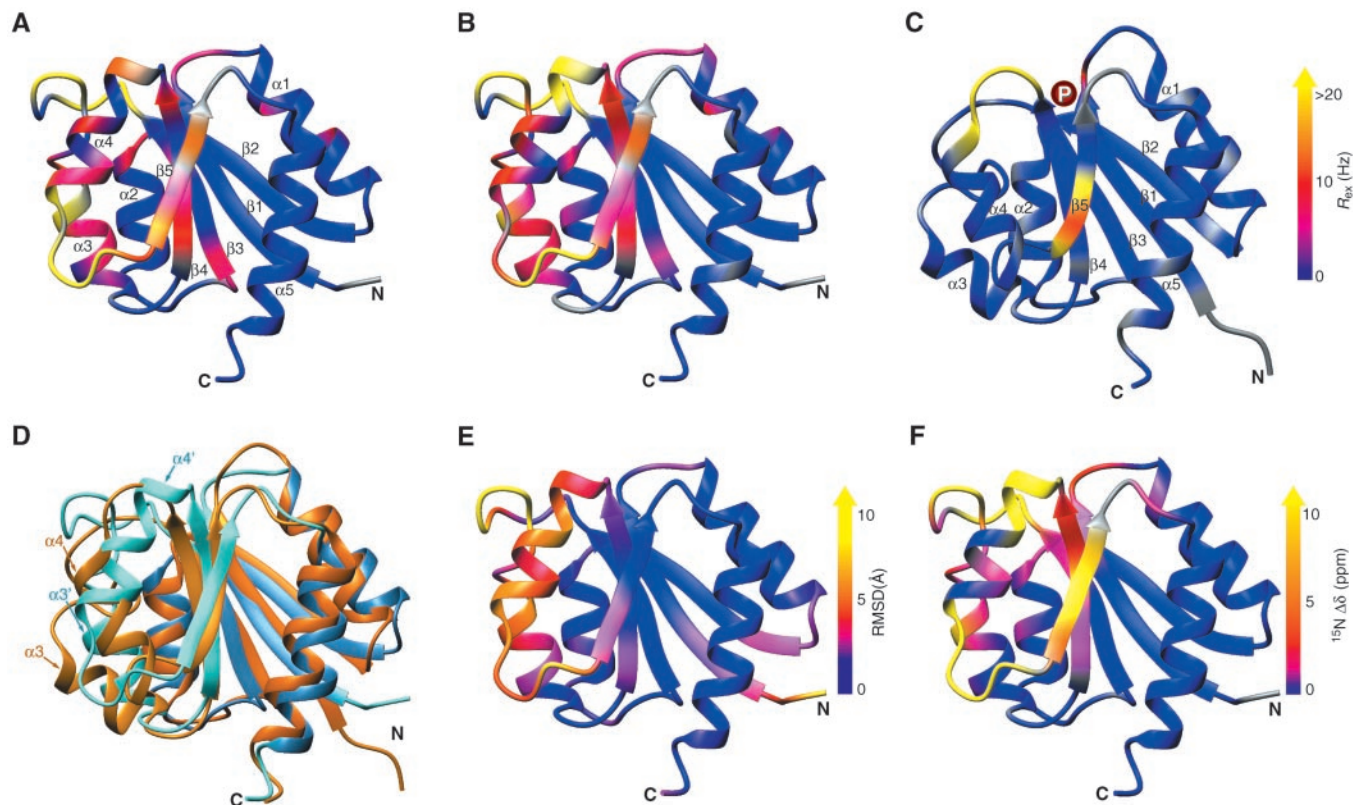
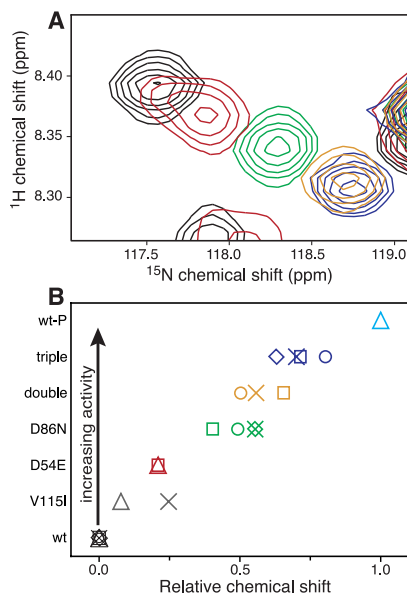


Fig. 3. Color-coded representation of the conformational exchange dynamics, structural rearrangement, and chemical shift perturbations related to NtrC^c activation. Values of R_{ex} (Fig. 2B) are indicated on a ribbon diagram with a continuous color scale for (A) NtrC^c, (B) NtrC^c(D86N/A89T), and (C) P-NtrC^c. (D) The NMR structures of NtrC^c (cyan/blue) and P-NtrC^c (yellow/orange) are superimposed using residues 4 to 9, 14 to 53, and 108 to 121, indicated in darker colors (orange and blue), with the

structural differences highlighted in lighter colors (yellow and cyan) (8). (E) This structural rearrangement upon phosphorylation is presented as backbone RMS deviations (Fig. 2C) in a continuous color scale. (F) Chemical shift perturbations due to phosphorylation of NtrC^c (Fig. 2C) are displayed in a similar manner. All structural representations were generated in MOLMOL using Protein Data Bank entries 1DC7 for NtrC^c (A, B, and D through F) and 1DC8 for P-NtrC^c (C and D).

Fig. 4. Relationship between chemical shift changes and activity of the following NtrC^c forms (36): V115I (gray), D54E (red), D86N (green), D86N/A89T (gold), D86N/A89T/V115I (blue), and P-NtrC^c (cyan) in respect to wild-type NtrC^c (black). (A) Signals for D88 in ^1H - ^{15}N HSQC spectra of five NtrC variants are superimposed. Larger chemical shift changes (shift of the signal to the lower right corner) coincide with increased activity of the corresponding mutants (10). This collinear shift behavior is observed for a number of residues, as shown in (B): D88 (□), D11 (○), D10 (×), M81 (◇), and V91 (△). Chemical shifts are shown relative to P-NtrC^c and therefore reflect the relative population between inactive and active conformers for each mutant.



Estimates of the overall rotational correlation times for each sample were obtained from the R_2/R_1 ratios: 6.9, 7.5, and 11.1 ns for NtrC^c, NtrC^c(D86N/A89T), and P-NtrC^c, respectively. Model-free parameters were calculated using the program ModelFree version 4.01 (provided by A. G. Palmer). For each residue, the

following five combinations of model-free parameters were fit to the relaxation values along with the initial estimate of rotational correlation time (14, 15): (1) S^2 , (2) S^2 and τ_e , (3) S^2 and R_{ex} , (4) S^2 , τ_e , and R_{ex} , and (5) S^2 , τ_e , and S^2_f , where model 5 takes explicit account of fast (pico- to nanosecond) mo-

tions on two distinct time scales. Model selection was performed as described (30) using an isotropic diffusion model. In all three forms of NtrC^c, the relaxation data for most residues were analyzed using either a one-parameter (S^2) or two-parameter (S^2 and τ_e , or S^2 and R_{ex}) model. Model-free fits to the relaxation data were optimized simultaneously including the overall rotational correlation time (τ_m) as a global variable. Final τ_m values are 6.5, 7.21, and 10.9 ns for NtrC^c, NtrC^c(D86N/A89T), and P-NtrC^c, respectively. The large correlation time of the phosphorylated form is primarily due to the high salt concentration for the phosphorylation reaction which increases the viscosity of the buffer by a factor of 1.4 compared to the buffer used for the unphosphorylated forms (8). That dimerization or aggregation might be responsible for the variations in rotational tumbling was investigated by NMR self-diffusion and analytical ultracentrifugation measurements. In all instances, no evidence for dimer formation was observed (8). Despite this, increased viscosity fails to fully account for increases in τ_m for P-NtrC^c (20% remaining), and τ_m is also 10% larger for the double mutant compared to NtrC^c. This increase in correlation time may result from structural changes related to the activation process. The structure of activated NtrC^c reveals a hydrophobic face exposed by rotation of helix 4, and this dramatic change in solvent-accessible surface polarity may affect the behavior of the isolated domain in solution.

17. In extended model-free analysis of relaxation data, factors other than conformational exchange could give rise to an apparent contribution of R_{ex} , including anisotropic rotational diffusion or exchange between monomer and dimer species. Fits to the relaxation

REPORTS

- data for NtrC^c incorporating either anisotropic global diffusion (31) or local diffusion (32) provided no significant improvement or deviation from the results obtained with the isotropic model. Moreover, R_{ex} terms arising from unappreciated anisotropy should reside within a subset of bond vectors oriented along the axis of the protein rotating most slowly. This is not the case in either wild-type or double-mutant NtrC^c, where N–H bond vectors with R_{ex} have a broad angular distribution. Of the three NtrC^c species, the increased hydrophobic exposure of P-NtrC^c might be expected to promote dimerization or aggregation. Under experimental conditions, this could be excluded and in addition, R_{ex} virtually disappears for P-NtrC^c. That suggests that all three forms tumble isotropically and that the observed R_{ex} terms are due to conformational exchange on micro- to millisecond time scales.
18. S. Djordjevic, A. M. Stock, *J. Struct. Biol.* **124**, 189 (1998).
 19. R. E. Silversmith, R. B. Bourret, *Trends Microbiol.* **7**, 16 (1999).
 20. V. A. Feher, J. Cavanagh, *Nature* **400**, 289 (1999).
 21. It has been emphasized recently that observation of a single exchange-broadened resonance does not indicate per se that the exchange process is fast on the chemical-shift time scale ($k_{ex} \gg \Delta\omega$) (33, 34). However, this is only true for strongly skewed populations. Our data reflect the fast exchange regime because the populations of the two sites are similar for the mutant form and only a single set of resonances is observed.
 22. C. Wyman, I. Rombel, A. K. North, C. Bustamante, S. Kustu, *Science* **275**, 1658 (1997).
 23. A. K. North, S. Kustu, *J. Mol. Biol.* **267**, 17 (1997).
 24. R. Barak, M. Eisenbach, *Biochemistry* **31**, 1821 (1992).
 25. F. J. Moy *et al.*, *Biochemistry* **33**, 10731 (1994).
 26. The Web movie [http://bioinfo.mbb.yale.edu/mol-movdb; W. G. Krebs, M. Gerstein, *Nucleic Acids Res.* **28**, 1665 (2000)] is also available at www.sciencemag.org/cgi/content/full/291/5512/2429/DC1.
 27. An aromatic residue is highly conserved at this position among the receiver domain family (35), and its reorientation has been discussed to be an important element in CheY activation. However the correlation between function and the rotameric state of this conserved aromatic side chain is controversial (18, 19). Our structural and dynamic data on NtrC^c in three different functional states reveal that Y101 is mobile in both the "on" and "off" state in NtrC^c, which may explain the inconsistent results from the various CheY and SpoOF crystal structures. Crystallization may trap one of the accessible states, depending on the equilibrium and on the solution conditions. The presence of two modes of motion in NtrC^c shows that the simplest two-state model is not strictly accurate. The equilibrium constants between I and A can only qualitatively be estimated from the chemical shift and relaxation data because of (i) the two uncoupled motions present, (ii) additional chemical shift perturbation due to Mg²⁺ and phosphate binding in the active site and shift perturbation due to amino acid substitutions. These effects consequently result in a relatively weak correlation between R_{ex} and ¹⁵N shifts. Further studies are in progress to quantitatively dissect the two processes and to directly determine the rate constants.
 28. N. Tjandra, H. Kuboniwa, H. Ren, A. Bax, *Eur. J. Biochem.* **230**, 1014 (1995).
 29. A. Malmendal, J. Evenas, S. Forsen, M. Akke, *J. Mol. Biol.* **293**, 883 (1999).
 30. A. M. Mandel, M. Akke, A. G. I. Palmer, *J. Mol. Biol.* **246**, 144 (1995).
 31. L. Lee, M. Rance, W. J. Chazin, A. G. Palmer, *J. Biomol. NMR* **9**, 287 (1997).
 32. J. M. Schurr, H. P. Babcock, B. S. Fujimoto, *J. Magn. Reson. B* **105**, 211 (1994).
 33. O. Millet, J. P. Loria, C. D. Kroenke, M. Pons, A. G. Palmer, *J. Am. Chem. Soc.* **122**, 2867 (2000).
 34. R. Ishima, D. A. Torchia, *J. Biomol. NMR* **14**, 369 (1999).
 35. K. Volz, *Biochemistry* **32**, 11741 (1993).
 36. Single-letter abbreviations for the amino acid residues are as follows: A, Ala; D, Asp; E, Glu; I, Ile; M, Met; N, Asn; P, Pro; T, Thr; V, Val; and Y, Tyr.
 37. We gratefully acknowledge the assistance of A. G. Palmer with ModelFree 4.0 and S. Kustu for helpful discussions and plasmid DNA. Supported by NIH grant GM62117 to D.K. and instrumentation grants from the NSF; the Keck Foundation; and the Director, Office of Biological and Environmental Research, Office of Energy Research of the U.S. Department of Energy. NMR studies were carried out at the NMR-FAM with support from the NIH Biomedical Technology Program and additional equipment funding from the University of Wisconsin, NSF Academic Infrastructure Program, NIH Shared Instrumentation Program, NSF Biological Instrumentation Program, and U.S. Department of Agriculture. Relaxation data and dynamics parameters have been deposited in the BioMagResBank (www.bmrb.wisc.edu) under the accession codes 4762 for NtrC^c, 4763 for NtrC^c(D86N/A89T), and 4764 for P-NtrC^c.

13 December 2000; accepted 7 February 2001

Science ~~ONLINE~~

Take a hike!

In our Enhanced Perspectives, we navigate the virtual forest for you. Each week, one Perspective from *Science's* *Compass* links readers to the best related Web-based content:

- research databases
- tutorials
- glossaries
- abstracts
- other online material

Take your virtual hike at www.sciencemag.org/misc/e-perspectives.shtml